

# Study of baryon acoustic oscillations with SDSS DR12 data and measurements of $\Omega_k$ and $\Omega_{\text{DE}}(a)$ . Part II.

B. Hoeneisen<sup>1</sup>

<sup>1</sup>*Universidad San Francisco de Quito, Quito, Ecuador*

(Dated: August 31, 2016)

We define Baryon Acoustic Oscillation (BAO) observables  $\hat{d}_\alpha(z, z_c)$ ,  $\hat{d}_z(z, z_c)$ , and  $\hat{d}_\parallel(z, z_c)$  that do not depend on any cosmological parameter. From each of these observables we recover the BAO correlation length  $d_{\text{BAO}}$  with its respective dependence on cosmological parameters. These BAO observables are measured as a function of redshift  $z$  with the Sloan Digital Sky Survey (SDSS) data release DR12. From the BAO measurements alone, or together with the correlation angle  $\theta_{\text{MC}}$  of the Cosmic Microwave Background (CMB), we constrain the curvature parameter  $\Omega_k$  and the dark energy density  $\Omega_{\text{DE}}(a)$  as a function of the expansion parameter  $a$  in several scenarios. These observables are further constrained with external measurements of  $h$  and  $\Omega_b h^2$ . We find some tension between the data and a cosmology with flat space and constant dark energy density  $\Omega_{\text{DE}}(a)$ .

## INTRODUCTION

We present studies of baryon acoustic oscillations (BAO) with Sloan Digital Sky Survey (SDSS) data release DR12 [1]. Part I of this ongoing study is Ref. [2]. We refer the reader to Part I for the notation and methods. This is an outline of the study:

(i) We define and measure BAO observables  $\hat{d}_\alpha(z, z_c)$ ,  $\hat{d}_z(z, z_c)$ , and  $\hat{d}_\parallel(z, z_c)$  that do not depend on any cosmological parameter, see Part I [2]. From each of these observables we obtain the BAO correlation distance  $d_{\text{BAO}}$  with its respective dependence on the cosmological parameters. We present many redundant measurements with different galaxy selections, i.e. different background fluctuations, to gain confidence in the results.

(ii) We use the measured BAO distances, and the correlation angle  $\theta_{\text{MC}}$  of the Cosmic Microwave Background (CMB), as an uncalibrated standard ruler to constrain the correlated parameters  $\Omega_k$  and  $\Omega_{\text{DE}}(a)$ . The cosmological parameters  $h$ ,  $\Omega_b h^2$  and  $N_{\text{eff}}$  drop out of this analysis.

(iii) Finally we use the measured BAO distances and  $\theta_{\text{MC}}$  as a calibrated standard ruler to further constrain  $\Omega_k$  with external measurements of  $h$  and  $\Omega_b h^2$ .

The results of this analysis are compared with the final consensus results corresponding to the DR12 data [3].

## BAO DISTANCES IN THE NORTHERN AND SOUTHERN GALACTIC CAPS

To gain confidence in the identification of the BAO signal from among the background fluctuations, and to obtain the uncertainties by a different method, we repeat the measurements separately for galaxies in the northern and southern galactic caps. This time we analyze SDSS DR12 galaxies (passing the same quality selection flags and  $z_{\text{Err}} < 0.001$ ) with right as-

cension  $110^\circ$  to  $270^\circ$  and declination  $-5^\circ$  to  $70^\circ$  with  $17.0 < r_{35} < 27.0$ . The galactic plane separates this sample into two independent sub-samples defined by  $\text{dec} \geq 27.0^\circ - 17.0^\circ [(ra - 185.0^\circ)/(260.0^\circ - 185.0^\circ)]^2$ . These sub-samples are referred to as northern ( $>$ ) and southern ( $<$ ) galactic caps. The results of measurements for G-G and G-C runs are presented in Tables I and II. Blank entries indicate that we were unable to reliably identify a BAO signal.

We combine the measurements of the two independent sub-samples as follows: (i) if fits are successful for both G-G and G-C runs we take the arithmetic average of the two measurements; (ii) we then take the arithmetic average of each corresponding measurement for the northern and southern galactic caps, and assign to each of these averages an independent total uncertainty  $\sigma$  equal to half the total root-mean-square (r.m.s.) difference of all measurements in the northern and southern galactic caps; and finally, (iv) assign an independent systematic uncertainty  $\sqrt{2}\sigma$  to each entry in Tables I and II. This procedure obtains almost the same uncertainties as the method used for Table III of Part I [2] in spite of the fact that there are more galaxies in the northern galactic cap than in the southern galactic cap, i.e. we find larger background fluctuations in the north. The averages are summarized in Table III.

The two sets of measurements presented in Table III of Part I [2] and Table III have different background fluctuations due to galaxy clustering, have different fits, obtain uncertainties by different methods, and obtain essentially the same results and uncertainties. The root-mean-square of the differences of all entries in Table III of Part I [2] and Table III divided by  $\sqrt{2}$  is 0.00046 which is less than the total independent uncertainties assigned to each entry of each Table, so these measurements are consistent.

TABLE I: Measured BAO distances  $\hat{d}_\alpha(z, z_c)$ ,  $\hat{d}_z(z, z_c)$ , and  $\hat{d}_l(z, z_c)$  in units of  $c/H_0$  with  $z_c = 3.79$  (see Part I [2]) from SDSS DR12 galaxies with right ascension  $110^0$  to  $270^0$ , and declination  $-5^0$  to  $70^0$  in the northern galactic cap, i.e.  $\text{dec} > 27.0^0 - 17.0^0 \left[ (\text{ra} - 185.0^0)/(260.0^0 - 185.0^0) \right]^2$ . Uncertainties are statistical from the fits to the BAO signal. Each BAO distance has an independent systematic uncertainty  $\pm 0.00085$ . No corrections have been applied.

$z$	$z_{\min}$	$z_{\max}$	galaxies	centers	type	$100\hat{d}_\alpha(z, z_c)$	$100\hat{d}_z(z, z_c)$	$100\hat{d}_l(z, z_c)$
0.10	0.0	0.2	187485	187485	G-G			
0.10	0.0	0.2	184044	27485	G-C	$3.434 \pm 0.008$		$3.340 \pm 0.013$
0.25	0.2	0.3	38672	38672	G-G			$3.369 \pm 0.012$
0.25	0.2	0.3	38657	22079	G-C	$3.284 \pm 0.013$	$3.223 \pm 0.013$	$3.334 \pm 0.009$
0.35	0.3	0.4	53462	53462	G-G	$3.246 \pm 0.016$	$3.210 \pm 0.013$	$3.295 \pm 0.009$
0.35	0.3	0.4	53461	24360	G-C	$3.324 \pm 0.009$	$3.376 \pm 0.015$	$3.288 \pm 0.010$
0.46	0.4	0.5	86528	86528	G-G	$3.538 \pm 0.009$		$3.483 \pm 0.023$
0.46	0.4	0.5	86528	21379	G-C	$3.487 \pm 0.004$	$3.319 \pm 0.011$	$3.458 \pm 0.015$
0.54	0.5	0.6	116301	116301	G-G	$3.380 \pm 0.010$	$3.486 \pm 0.011$	$3.583 \pm 0.013$
0.54	0.5	0.6	116301	19901	G-C	$3.460 \pm 0.014$	$3.471 \pm 0.014$	$3.509 \pm 0.014$
0.67	0.6	0.9	67772	67772	G-G	$3.360 \pm 0.030$		$3.451 \pm 0.013$
0.67	0.6	0.9	67772	3800	G-C	$3.273 \pm 0.012$		$3.492 \pm 0.015$
0.20	0.10	0.35	160471	160471	G-G			
0.20	0.10	0.35	160471	59392	G-C			$3.295 \pm 0.011$
0.47	0.35	0.55	178246	178246	G-G	$3.419 \pm 0.017$	$3.285 \pm 0.015$	$3.486 \pm 0.010$
0.46	0.35	0.55	178246	45592	G-C	$3.489 \pm 0.008$	$3.350 \pm 0.010$	$3.462 \pm 0.008$
0.63	0.55	0.90	119449	119449	G-G			$3.512 \pm 0.022$
0.63	0.55	0.90	119449	12003	G-C			

TABLE II: Measured BAO distances  $\hat{d}_\alpha(z, z_c)$ ,  $\hat{d}_z(z, z_c)$ , and  $\hat{d}_l(z, z_c)$  in units of  $c/H_0$  with  $z_c = 3.79$  (see Part I [2]) from SDSS DR12 galaxies with right ascension  $110^0$  to  $270^0$ , and declination  $-5^0$  to  $70^0$  in the southern galactic cap, i.e.  $\text{dec} < 27.0^0 - 17.0^0 \left[ (\text{ra} - 185.0^0)/(260.0^0 - 185.0^0) \right]^2$ . Uncertainties are statistical from the fits to the BAO signal. Each BAO distance has an independent systematic uncertainty  $\pm 0.00085$ . No corrections have been applied.

$z$	$z_{\min}$	$z_{\max}$	galaxies	centers	type	$100\hat{d}_\alpha(z, z_c)$	$100\hat{d}_z(z, z_c)$	$100\hat{d}_l(z, z_c)$
0.10	0.0	0.2	103008	103008	G-G			
0.10	0.0	0.2	117786	14802	G-C	$3.262 \pm 0.009$	$3.350 \pm 0.013$	$3.351 \pm 0.003$
0.25	0.2	0.3	21112	21112	G-G	$3.420 \pm 0.019$	$3.307 \pm 0.008$	$3.529 \pm 0.010$
0.25	0.2	0.3	21108	11320	G-C	$3.473 \pm 0.012$	$3.292 \pm 0.010$	$3.504 \pm 0.009$
0.35	0.3	0.4	29739	29739	G-G	$3.408 \pm 0.032$	$3.347 \pm 0.016$	$3.464 \pm 0.031$
0.35	0.3	0.4	29739	12907	G-C	$3.388 \pm 0.010$	$3.327 \pm 0.010$	$3.463 \pm 0.011$
0.46	0.4	0.5	46447	46447	G-G	$3.501 \pm 0.015$		$3.280 \pm 0.027$
0.46	0.4	0.5	46447	9410	G-C			
0.54	0.5	0.6	65217	65217	G-G	$3.302 \pm 0.022$	$3.375 \pm 0.027$	$3.416 \pm 0.016$
0.54	0.5	0.6	65217	9943	G-C			
0.67	0.6	0.9	35100	35100	G-G	$3.438 \pm 0.014$		$3.399 \pm 0.018$
0.67	0.6	0.9	35100	1494	G-C			
0.19	0.10	0.35	92687	92687	G-G			
0.19	0.10	0.35	92687	30798	G-C	$3.338 \pm 0.010$		
0.47	0.35	0.55	98467	98467	G-G			$3.481 \pm 0.015$
0.47	0.35	0.55	98467	22063	G-C	$3.604 \pm 0.008$	$3.357 \pm 0.023$	$3.497 \pm 0.012$
0.62	0.55	0.90	63441	63441	G-G	$3.326 \pm 0.022$		$3.384 \pm 0.016$
0.62	0.55	0.90	63441	5389	G-C			$3.406 \pm 0.009$

## CORRECTIONS

Let us consider corrections to the BAO distances due to peculiar velocities and peculiar displacements of galaxies towards their centers. A relative peculiar velocity  $v_p$  towards the center causes a reduction of the BAO distances  $\hat{d}_\alpha(z, z_c)$ ,  $\hat{d}_z(z, z_c)$ , and  $\hat{d}_l(z, z_c)$  of order  $0.5v_p/c$ . In addition, the Doppler shift produces an apparent shortening

of  $\hat{d}_z(z, z_c)$  by  $v_p/c$ , and somewhat less for  $\hat{d}_l(z, z_c)$ .

We multiply the measured BAO distances  $\hat{d}_\alpha(z, z_c)$ ,  $\hat{d}_z(z, z_c)$ , and  $\hat{d}_l(z, z_c)$  by correction factors  $f_\alpha$ ,  $f_z$  and  $f_l$  respectively. Simulations in Ref. [4] obtain  $f_\alpha - 1 = 0.2283 \pm 0.0609\%$  and  $f_z - 1 = 0.2661 \pm 0.0820\%$  at  $z = 0.3$ ,  $f_\alpha - 1 = 0.1286 \pm 0.0425\%$  and  $f_z - 1 = 0.1585 \pm 0.0611\%$  at  $z = 1$ , and  $f_\alpha - 1 = 0.0435 \pm 0.0293\%$  and  $f_z - 1 = 0.0582 \pm 0.0402\%$  at  $z = 3$ . In the following

TABLE III: Independent measured BAO distances  $\hat{d}_\alpha(z, z_c)$ ,  $\hat{d}_z(z, z_c)$ , and  $\hat{d}_l(z, z_c)$  in units of  $c/H_0$  with  $z_c = 3.79$  (see Part I [2]) obtained by averaging measurements in the northern and southern galactic caps. Each BAO distance has an independent total uncertainty  $\pm 0.00060$  dominated by systematics. No corrections have been applied.

$z$	$z_{\min}$	$z_{\max}$	$100\hat{d}_\alpha(z, z_c)$	$100\hat{d}_z(z, z_c)$	$100\hat{d}_l(z, z_c)$
0.10	0.0	0.2	3.348	3.350	3.346
0.25	0.2	0.3	3.365	3.261	3.434
0.35	0.3	0.4	3.342	3.315	3.378
0.46	0.4	0.5	3.507	3.319	3.375
0.54	0.5	0.6	3.361	3.427	3.481
0.67	0.6	0.9	3.377		3.435

sections we present fits with the corrections

$$\begin{aligned} f_\alpha - 1 &= 0.320\% a^{1.35}, \\ f_z - 1 &= 0.381\% a^{1.35}, \\ f_l - 1 &= 0.350\% a^{1.35}. \end{aligned} \quad (1)$$

The effect of these corrections can be seen by comparing the first two fits in Table V below. Fits with corrections  $\sim 15$  times larger, or no corrections at all, are presented in Part I [2]. An order-of-magnitude estimate of this correction can be obtained by calculating the r.m.s.  $v_p$  corresponding to modes with  $k \equiv 2\pi/\lambda < 2\pi/(4d'_{\text{BAO}})$  with Eq. (11) of Ref. [5] and normalizing the result to  $\sigma_8$ , i.e. to the r.m.s. density fluctuation in a volume  $(8\text{Mpc}/h)^3$ .

## COMPARISON WITH THE FINAL CONSENSUS DR12 ANALYSIS

We compare the measured BAO observables in Table III of Part I [2] and Table III with the final consensus “BAO+FS” analysis of the DR12 data set [3] which is summarized in Table IV. The notation of Ref. [3] is related to our notation as follows:

$$\begin{aligned} D_M \frac{r_{\text{d,fid}}}{r_{\text{d}}} &= \frac{c}{H_0} \chi(z) \frac{r_{\text{d,fid}}}{d_{\text{BAO}}} \\ &= \frac{c}{H_0} r_{\text{d,fid}} \frac{z \exp(-z/z_c)}{\hat{d}_\alpha(z, z_c)}, \end{aligned} \quad (2)$$

$$\begin{aligned} H \frac{r_{\text{d}}}{r_{\text{d,fid}}} &= H_0 E(z) \frac{d_{\text{BAO}}}{r_{\text{d,fid}}} \\ &= \frac{H_0}{r_{\text{d,fid}}} \frac{\hat{d}_z(z, z_c)}{(1 - z/z_c) \exp(-z/z_c)}, \end{aligned} \quad (3)$$

where  $r_{\text{d,fid}} = 147.78 \text{ Mpc}$  and  $H_0 = 67.8 \pm 1.2 \text{ km s}^{-1} \text{ Mpc}^{-1}$ . We find agreement within the quoted uncertainties between our measurements in Tables III of Part I [2] or III and the final consensus measurements in Table IV.

Table IV also shows  $\Omega_{\text{DE}}(z)$  extracted from  $H$  with  $\Omega_k = 0$  and  $\Omega_{\text{m}} = 0.310 \pm 0.005$  [3]. These values of  $\Omega_{\text{DE}}(z)$  are in agreement with our results in Fig. 2 below. The observed increase of  $\Omega_{\text{DE}}(z)$  with  $z$  was studied in Part I [2].

## CONSTRAINTS ON $\Omega_k$ AND $\Omega_{\text{DE}}(a)$ FROM UNCALIBRATED BAO

Let us try to understand qualitatively how the BAO distance measurements presented in Table III constrain the cosmological parameters. In the limit  $z \rightarrow 0$  we obtain  $d_{\text{BAO}} = \hat{d}_\alpha(0, z_c) = \hat{d}_z(0, z_c) = \hat{d}_l(0, z_c)$ , so the row with  $z = 0.1$  in Table III approximately determines  $d_{\text{BAO}}$ . This  $d_{\text{BAO}}$  and the measurement of, for example,  $\hat{d}_z(0.3, z_c)$  then constrains the derivative of  $\Omega_{\text{m}}/a^3 + \Omega_{\text{DE}} + \Omega_k/a^2$  with respect to  $a$  at  $z \approx 0.3$ , i.e. constrains approximately  $\Omega_{\text{DE}} + 0.5\Omega_k$  or equivalently  $\Omega_{\text{DE}} - \Omega_{\text{m}}$ . We need an additional constraint for Scenario 1. At small  $a$ ,  $E(a)$  is dominated by  $\Omega_{\text{m}}$ , so  $\theta_{\text{MC}}$  plus  $d_{\text{BAO}}$  approximately constrain  $\Omega_{\text{m}}$ , or equivalently  $\Omega_{\text{DE}} + \Omega_k$ , see Eq. (19) of Part I [2]. The additional BAO distance measurements in Table III then also constrain  $w_0$  and  $w_a$  or  $w_1$ .

We now constrain cosmological parameters with each of these three sets of independent BAO measurements: 18 BAO distances in Table III of Part I [2], 12 BAO distances in Table IV of Part I (rows with  $0.2 < z < 0.4$  G-C,  $0.4 < z < 0.5$  G-C,  $0.5 < z < 0.6$  G-LC, and  $0.6 < z < 0.9$  LG-LG), or 17 BAO distances in Table III.

In Table V we present the cosmological parameters obtained by minimizing the  $\chi^2$  with 17 terms corresponding to the 17 BAO distance measurements in Table III for several scenarios. We find that the data is in agreement with the simplest cosmology with  $\Omega_k = 0$  and  $\Omega_{\text{DE}}(a)$  constant with  $\chi^2$  per degree of freedom (d.f.) 15.4/15, so no additional parameter is needed to obtain a good fit to this data.

For the sets of 18, 12 or 17 BAO measurements we obtain, respectively,  $\Omega_{\text{DE}} + 0.6\Omega_k = 0.620 \pm 0.030$ ,  $0.652 \pm 0.041$ , and  $0.647 \pm 0.031$  for constant  $\Omega_{\text{DE}}(a)$ , or  $0.638 \pm 0.058$ ,  $0.585 \pm 0.063$ , and  $0.627 \pm 0.075$  if  $\Omega_{\text{DE}}(a)$  is allowed to depend on  $a$  as in Scenario 4. We present the variable  $\Omega_{\text{DE}} + 0.6\Omega_k$  instead of  $\Omega_{\text{DE}}$  because it has a smaller uncertainty. The constraints on  $\Omega_k$  are weak.

In Table VI we present the cosmological parameters obtained by minimizing the  $\chi^2$  with 19 terms corresponding to the 18 BAO distance measurements listed in Table III of Part I [2] plus the correlation angle  $\theta_{\text{MC}} = 0.010413 \pm 0.000006$  of the CMB [6]. We present the variable  $\Omega_{\text{DE}} + 2\Omega_k$  instead of  $\Omega_{\text{DE}}$  because it has a smaller uncertainty. The corresponding fits for the 17 BAO measurements of Table III plus  $\theta_{\text{MC}}$  are presented in Table VII.

From the fits for  $\theta_{\text{MC}}$  plus the set of 18, or 12 or

TABLE IV: Final consensus “BAO+FS” measurements of the DR12 data set [3] (uncertainties are statistical and systematic), and the corresponding BAO parameters  $\hat{d}_\alpha(z, z_c)$  and  $\hat{d}_z(z, z_c)$  with  $z_c = 3.79$ . These measurements include the peculiar motion corrections. For comparison, the quoted errors on  $\hat{d}_\alpha(z, z_c)$  and  $\hat{d}_z(z, z_c)$  exclude the uncertainty of  $H_0$ . Also shown is  $\Omega_{\text{DE}}(z)$  extracted from  $H$  with  $\Omega_k = 0$  and  $\Omega_m = 0.310 \pm 0.005$  [3] with uncorrelated and correlated uncertainties.

$z$	$D_M r_{\text{d, fid}}/r_{\text{d}}$ [Mpc]	$100\hat{d}_\alpha(z, z_c)$	$H r_{\text{d}}/r_{\text{d, fid}}$ [km s <sup>-1</sup> Mpc <sup>-1</sup> ]	$100\hat{d}_z(z, z_c)$	$\Omega_{\text{DE}}(z)$
0.38	$1518 \pm 20 \pm 11$	$3.346 \pm 0.050$	$81.5 \pm 1.7 \pm 0.9$	$3.270 \pm 0.077$	$0.698 \pm 0.071$ (uncorr) $\pm 0.058$ (corr)
0.51	$1977 \pm 23 \pm 14$	$3.332 \pm 0.045$	$90.5 \pm 1.7 \pm 1.0$	$3.375 \pm 0.074$	$0.798 \pm 0.081$ (uncorr) $\pm 0.070$ (corr)
0.61	$2283 \pm 28 \pm 16$	$3.362 \pm 0.047$	$97.3 \pm 1.8 \pm 1.1$	$3.426 \pm 0.061$	$0.862 \pm 0.077$ (uncorr) $\pm 0.081$ (corr)

TABLE V: Cosmological parameters obtained from the 17 BAO measurements in Table III in several scenarios. Corrections for peculiar motions are given by Eq. (1) except, for comparison, the fit “1\*” which has no correction. Scenario 1 has  $\Omega_{\text{DE}}(a)$  constant. Scenario 3 has  $w = w_0$ . Scenario 4 has  $\Omega_{\text{DE}}(a) = \Omega_{\text{DE}}[1 + w_1(1 - a)]$ .

	Scenario 1*	Scenario 1	Scenario 1	Scenario 3	Scenario 4	Scenario 4
$\Omega_k$	0 fixed	0 fixed	$-0.413 \pm 0.234$	0 fixed	0 fixed	$-0.377 \pm 0.263$
$\Omega_{\text{DE}} + 0.6\Omega_k$	$0.680 \pm 0.023$	$0.682 \pm 0.023$	$0.647 \pm 0.031$	$0.614 \pm 0.051$	$0.611 \pm 0.073$	$0.627 \pm 0.075$
$w_0$	n.a.	n.a.	n.a.	$-1.346 \pm 0.349$	n.a.	n.a.
$w_a$ or $w_1$	n.a.	n.a.	n.a.	n.a.	$-1.075 \pm 1.159$	$-0.244 \pm 0.894$
$100d_{\text{BAO}}$	$3.37 \pm 0.03$	$3.38 \pm 0.03$	$3.40 \pm 0.03$	$3.44 \pm 0.07$	$3.44 \pm 0.07$	$3.42 \pm 0.07$
$\chi^2/\text{d.f.}$	15.6/15	15.4/15	12.5/14	14.3/14	14.3/14	12.4/13

17 BAO measurements we obtain, respectively,  $\Omega_{\text{DE}} + 2\Omega_k = 0.718 \pm 0.006$ ,  $0.749 \pm 0.024$ , or  $0.717 \pm 0.007$  when  $\Omega_{\text{DE}}(a)$  is allowed to vary as in Scenario 4. The constraints on  $\Omega_k$  are, respectively,  $0.037 \pm 0.011$ ,  $0.043 \pm 0.015$ , or  $0.022 \pm 0.012$  for constant  $\Omega_{\text{DE}}(a)$ , or  $0.044 \pm 0.041$ ,  $0.116 \pm 0.057$ , or  $0.060 \pm 0.052$  when  $\Omega_{\text{DE}}(a)$  is allowed to vary as in Scenario 4. The constraints on  $w_1$  are respectively  $0.74 \pm 0.24$ ,  $1.00 \pm 0.40$ , or  $0.38 \pm 0.23$  for  $\Omega_k = 0$ .

Note that the BAO plus  $\theta_{\text{MC}}$  data is consistent with  $\Omega_k = 0$  or with constant  $\Omega_{\text{DE}}(a)$ , i.e.  $w_1 = 0$ , but there is some tension when both constraints are applied. A summary of tensions is presented in Table VIII. The tension is not statistically significant for the 17 BAO plus  $\theta_{\text{MC}}$  data (in part because the 17 BAO set has no measurement of  $\hat{d}_z(0.67, z_c)$ , see Figures 1 and 2 below).

### MEASUREMENT OF $\Omega_{\text{DE}}(a)$

We obtain  $\Omega_{\text{DE}}(a)$  from the 5 independent measurements of  $\hat{d}_z(z, z_c)$  in Table III and Eqs. (17) and (2) of Part I [2], for the case  $\Omega_k = 0$ . The values of  $d_{\text{BAO}}$  and  $\Omega_m = 1 - \Omega_{\text{DE}} - \Omega_k$  are obtained from the fit for Scenario 4 in Table VII. The results are presented in Fig. 1. To guide the eye, we also show the straight line corresponding to the central values of  $\Omega_{\text{DE}}$  and  $w_1$  of the fit for Scenario 4.

To check the robustness of  $\Omega_{\text{DE}}(a)$  in Fig. 1 we add the 6 measurements of  $\hat{d}_z(z, z_c)$  in Table III of Part I [2] and the 17 measurements of  $\hat{d}_z(z, z_c)$  in Table IV of Part I and obtain Fig. 2. Note that these measurements

of  $\hat{d}_z(z, z_c)$  are partially correlated. Note that there is tension with a constant  $\Omega_{\text{DE}}(a)$  for  $0.6 < a < 0.67$ . Note also that the final consensus measurements of DR12 [3] in the last column of Table IV are in agreement with Fig. 2, and also show the tension with  $\Omega_k = 0$  and constant  $\Omega_{\text{DE}}(a)$ .

We repeat these two figures for the fit for Scenario 1 in Table VII, see Figs. 3 and 4. For these figures  $\Omega_k = 0.0218$ . The excesses of  $\Omega_{\text{DE}}(a)$  for  $0.6 < a < 0.67$  are not understood.

### CONSTRAINTS ON $\Omega_k$ AND $\Omega_{\text{DE}}(a)$ FROM CALIBRATED BAO

Up to this point we have used the BAO distance  $d_{\text{BAO}}$  as an uncalibrated standard ruler. The cosmological parameters  $h$ ,  $\Omega_b h^2$  and  $N_{\text{eff}}$  drop out of such an analysis. In this Section we consider the BAO distance  $d_{\text{BAO}} = r_s$  as a calibrated standard ruler and use independently measured  $h$  and  $\Omega_b h^2$ , while keeping  $N_{\text{eff}} = 3.36$  fixed, to further constrain the cosmological parameters.

The sound horizon is calculated from first principles [7] as follows:

$$r'_S = \int_0^{t_{\text{dec}}} \frac{c_s dt}{a} = \int_0^{a_{\text{dec}}} \frac{c_s da}{H_0 a^2 E(a)}, \quad (4)$$

where the speed of sound is

$$c_s = \frac{c}{\sqrt{3(1 + 3\rho_{b0}a/(4\rho_{\gamma 0})}}. \quad (5)$$

TABLE VI: Cosmological parameters obtained from the 18 BAO measurements in Table III of Part I [2] plus  $\theta_{\text{MC}}$  in several scenarios. Corrections for peculiar motions are given by Eq. (1). Scenario 1 has  $\Omega_{\text{DE}}(a)$  constant. Scenario 2 has  $w(a) = w_0 + w_a(1 - a)$ . Scenario 3 has  $w = w_0$ . Scenario 4 has  $\Omega_{\text{DE}}(a) = \Omega_{\text{DE}} [1 + w_1(1 - a)]$ .

	Scenario 1	Scenario 1	Scenario 2	Scenario 3	Scenario 4	Scenario 4
$\Omega_k$	0 fixed	$0.037 \pm 0.011$	0 fixed	0 fixed	0 fixed	$0.044 \pm 0.041$
$\Omega_{\text{DE}} + 2\Omega_k$	$0.735 \pm 0.004$	$0.718 \pm 0.006$	$0.780 \pm 0.082$	$0.726 \pm 0.005$	$0.720 \pm 0.006$	$0.718 \pm 0.006$
$w_0$	n.a.	n.a.	$-0.904 \pm 0.107$	$-0.815 \pm 0.051$	n.a.	n.a.
$w_a$ or $w_1$	n.a.	n.a.	$0.824 \pm 0.257$	n.a.	$0.736 \pm 0.235$	$-0.173 \pm 0.940$
$100d_{\text{BAO}}$	$3.47 \pm 0.02$	$3.39 \pm 0.03$	$3.40 \pm 0.05$	$3.36 \pm 0.04$	$3.35 \pm 0.04$	$3.40 \pm 0.06$
$\chi^2/\text{d.f.}$	36.7/17	23.6/16	23.0/15	24.0/16	24.8/16	23.6/15

TABLE VII: Cosmological parameters obtained from the 17 BAO measurements in Table III plus  $\theta_{\text{MC}}$  in several scenarios. Corrections for peculiar motions are given by Eq. (1). Scenario 1 has  $\Omega_{\text{DE}}(a)$  constant. Scenario 2 has  $w(a) = w_0 + w_a(1 - a)$ . Scenario 3 has  $w = w_0$ . Scenario 4 has  $\Omega_{\text{DE}}(a) = \Omega_{\text{DE}} [1 + w_1(1 - a)]$ .

	Scenario 1	Scenario 1	Scenario 2	Scenario 3	Scenario 4	Scenario 4
$\Omega_k$	0 fixed	$0.022 \pm 0.012$	0 fixed	0 fixed	0 fixed	$0.060 \pm 0.052$
$\Omega_{\text{DE}} + 2\Omega_k$	$0.727 \pm 0.004$	$0.716 \pm 0.007$	$0.767 \pm 0.071$	$0.721 \pm 0.005$	$0.719 \pm 0.006$	$0.717 \pm 0.007$
$w_0$	n.a.	n.a.	$-0.997 \pm 0.103$	$-0.895 \pm 0.056$	n.a.	n.a.
$w_a$ or $w_1$	n.a.	n.a.	$0.920 \pm 0.318$	n.a.	$0.381 \pm 0.229$	$-0.863 \pm 1.254$
$100d_{\text{BAO}}$	$3.43 \pm 0.02$	$3.38 \pm 0.03$	$3.41 \pm 0.05$	$3.37 \pm 0.04$	$3.37 \pm 0.04$	$3.43 \pm 0.07$
$\chi^2/\text{d.f.}$	19.5/16	15.7/15	15.0/14	16.1/15	16.4/15	15.1/14

TABLE VIII: There is some tension between the data and fits with  $\Omega_k = 0$  and  $\Omega_{\text{DE}}(a)$  constant, i.e.  $w_1 = 0$  in Scenario 4. Shown is the reduction of the  $\chi^2$  of the fits when either  $\Omega_k$  or  $w_1$  is released. The BAO measurements correspond to Tables III or IV of Part I [2], or Table III. Entries with \* have no significant tension with  $\Omega_k = 0$  and constant  $\Omega_{\text{DE}}(a)$ .

Reduction of $\chi^2$ by releasing	$\Omega_k$	$w_1$
Data:		
18 BAO + $\theta_{\text{MC}}$	13.1	11.9
12 BAO + $\theta_{\text{MC}}$	10.8	8.9
17 BAO + $\theta_{\text{MC}}$ *	3.8	3.1
18 BAO + $\theta_{\text{MC}}$ + $A = 1.000 \pm 0.022$	12.7	10.4
12 BAO + $\theta_{\text{MC}}$ + $A = 1.000 \pm 0.022$	9.8	6.9
17 BAO + $\theta_{\text{MC}}$ + $A = 1.000 \pm 0.022$ *	4.0	2.3
18 BAO + $\theta_{\text{MC}}$ + $A = 0.968 \pm 0.012$	4.9	16.3
12 BAO + $\theta_{\text{MC}}$ + $A = 0.968 \pm 0.012$	2.2	16.7
17 BAO + $\theta_{\text{MC}}$ + $A = 0.968 \pm 0.012$	0.6	5.7

We can write the result for our purposes as

$$r_S = 0.03389 \times A \times \left( \frac{0.30}{O_m} \right)^{0.255} \quad (6)$$

where

$$A = \left( \frac{h}{0.72} \right)^{0.489} \left( \frac{0.023}{\Omega_b h^2} \right)^{0.098} \left( \frac{3.36}{N_{\text{eff}}} \right)^{0.245} \quad (7)$$

(we have neglected the dependence of  $z_{\text{dec}} = 1090.2 \pm 0.7$  on the cosmological parameters). We take  $\Omega_b h^2 = 0.023 \pm 0.002$  from Big-Bang nucleosynthesis [6]. With the latest direct measurement  $h = 0.720 \pm 0.030$  by the HUB-

BLE satellite [8] we obtain  $A = 1.000 \pm 0.022$ . The alternative value  $h = 0.673 \pm 0.012$  is obtained from PLANK + WP + highL [6] assuming  $\Omega_k = 0$  and constant  $\Omega_{\text{DE}}(a)$ . For this  $h$  we obtain  $A = 0.968 \pm 0.012$ . The cosmological parameters that minimize the  $\chi^2$  with 19 terms (17 BAO measurements from Table III plus  $\theta_{\text{MC}}$  plus  $A$ ) are presented in Table IX.

From the fits to  $\theta_{\text{MC}}$  plus  $A$  plus each of the sets of 18, 12 or 17 BAO measurements we obtain, for free  $\Omega_{\text{DE}}(a)$  as in Scenario 4,  $\Omega_k = 0.027 \pm 0.018$ ,  $0.031 \pm 0.019$ , and  $0.023 \pm 0.019$  for  $A = 1.000 \pm 0.022$ , and  $0.001 \pm 0.010$ ,  $0.006 \pm 0.012$ , and  $-0.004 \pm 0.010$  for  $A = 0.968 \pm 0.012$ . Note that the external constraint from  $A$  reduces the uncertainty on  $\Omega_k$ .

## CONCLUSIONS

The results of these studies are:

(i) We define and measure BAO observables  $\hat{d}_\alpha(z, z_c)$ ,  $\hat{d}_z(z, z_c)$ , and  $\hat{d}_\parallel(z, z_c)$  that do not depend on any cosmological parameter. From each of these observables we obtain the BAO correlation distance  $d_{\text{BAO}}$  in units of  $c/H_0$  with its respective dependence on the cosmological parameters. It is difficult to distinguish the BAO signal from the background fluctuations due to the clustering of galaxies. To gain confidence in the results we repeat the measurements many times with different galaxy selections to obtain different background fluctuations. The measured BAO observables in Tables III and IV of Part I [2] and Table III are the main result of these studies. These measurements in combination with independent

TABLE IX: Cosmological parameters obtained from the 17 BAO measurements in Table III plus  $\theta_{MC}$  plus  $A$  in several scenarios. Corrections for peculiar motions are given by Eq. (1). Scenario 1 has  $\Omega_{DE}(a)$  constant. Scenario 4 has  $\Omega_{DE}(a) = \Omega_{DE}[1 + w_1(1 - a)]$ .

$A$	Scenario 1	Scenario 1	Scenario 4	Scenario 4	Scenario 4	Scenario 4
$\Omega_k$	$1.000 \pm 0.022$	$0.968 \pm 0.012$	$1.000 \pm 0.022$	$1.000 \pm 0.022$	$0.968 \pm 0.012$	$0.968 \pm 0.012$
$\Omega_{DE} + 2\Omega_k$	0 fixed	0 fixed	0 fixed	$0.023 \pm 0.019$	0 fixed	$-0.004 \pm 0.010$
$w_1$	n.a.	n.a.	$0.313 \pm 0.213$	$-0.049 \pm 0.377$	$0.457 \pm 0.201$	$0.488 \pm 0.212$
$100d_{BAO}$	$3.44 \pm 0.02$	$3.43 \pm 0.02$	$3.38 \pm 0.04$	$3.39 \pm 0.04$	$3.35 \pm 0.04$	$3.36 \pm 0.04$
$\chi^2/\text{d.f.}$	19.7/17	22.6/17	17.4/16	15.7/15	16.9/16	16.7/15

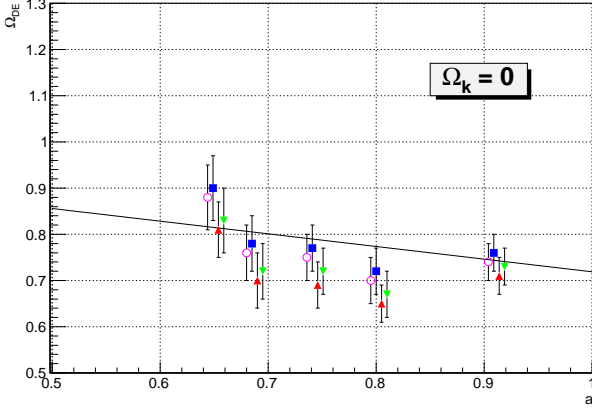


FIG. 1: Measurements of  $\Omega_{DE}(a)$  obtained from the 5  $\hat{d}_z(z, z_c)$  in Table III for  $\Omega_k = 0$ , and the corresponding  $d_{BAO}$  and  $\Omega_{DE}$  from the fit for Scenario 4 in Table VII. The straight line is  $\Omega_{DE}(a) = 0.7188[1 + 0.3813(1 - a)]$  from the central values of this fit. The uncertainties correspond only to the total uncertainties of  $\hat{d}_z(z, z_c)$ . For clarity some offsets in  $a$  have been applied. We present results for  $(d_{BAO}, \Omega_{DE}) = (0.03367, 0.7188)$  (squares),  $(0.03367 + 0.00044, 0.7188)$  (triangles),  $(0.03367, 0.7188 - 0.0063)$  (inverted triangles), and  $(0.03367, 0.7188 + 0.0063)$  (circles).

observations constrain cosmological parameters.

(ii) From the BAO measurements alone we obtain the constraint  $\Omega_{DE} + 0.6\Omega_k = 0.647 \pm 0.031$  for constant  $\Omega_{DE}(a)$ , or  $0.627 \pm 0.075$  when  $\Omega_{DE}(a)$  is allowed to depend on  $a$  as in Scenario 4. See Table V for fits in several scenarios.

(iii) From the BAO measurements plus  $\theta_{MC}$  from the CMB we obtain the constraints  $\Omega_{DE} + 2\Omega_k = 0.717 \pm 0.007$  and  $\Omega_k = 0.060 \pm 0.052$  when  $\Omega_{DE}(a)$  is allowed to vary as in Scenario 4. See Tables VI and VII for fits in several scenarios. The cosmological parameters  $h$ ,  $\Omega_b h^2$  and  $N_{\text{eff}}$  drop out of this analysis.

(iv) From the BAO measurements plus  $\theta_{MC}$  from the CMB plus external measurements of  $A$  defined in Eq. (7) we obtain  $\Omega_k = 0.023 \pm 0.019$  for  $A = 1.000 \pm 0.022$ ,

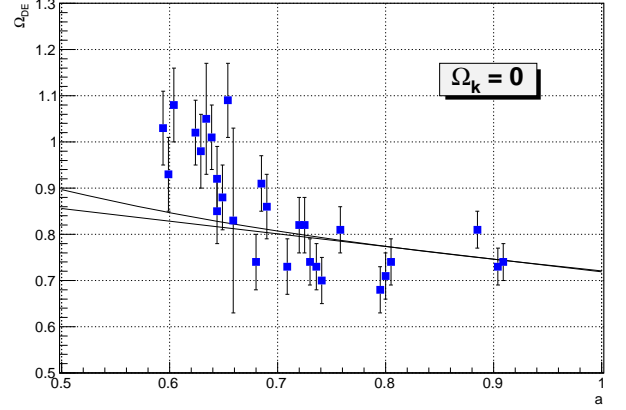


FIG. 2: Same as Figure 1 with the addition of the 6 measurements of  $\hat{d}_z(z, z_c)$  in Table III of Part I [2], and the 17 measurements of  $\hat{d}_z(z, z_c)$  in Table IV of Part I. These measurements are partially correlated. We present results for  $(d_{BAO}, \Omega_{DE}) = (0.03367, 0.7188)$ . The curve corresponding to the fit for Scenario 3 in Table VII has been added. The excesses of  $\Omega_{DE}(a)$  for  $0.6 < a < 0.67$  are not understood.

and  $-0.004 \pm 0.010$  for  $A = 0.968 \pm 0.012$ , when  $\Omega_{DE}(a)$  is allowed to vary as in Scenario 4. For more details see Table IX. Note that the external constraint from  $A$  reduces the uncertainty of  $\Omega_k$ .

(v) The data is consistent with the constraint  $\Omega_k = 0$  or the constraint  $\Omega_{DE}(a)$  constant, but there is some tension when both constraints are required. These tensions are presented in Table VIII and in Fig. 2. The measured excess of  $\Omega_{DE}(a)$  for  $0.6 < a < 0.67$  is not understood.

(vi) We note that the final consensus results of DR12 data [3] also show this tension, see last column in Table IV which is in agreement with Fig. 2. Finally we note that the BAO measurements in this study are in agreement with [3]: compare Table IV with Tables III or IV of Part I [2] or Table III. The two studies are complementary.

## ACKNOWLEDGMENT

Funding for SDSS-III has been provided by the Alfred P. Sloan Foundation, the Participating Institutions, the National Science Foundation, and the U.S. Department of Energy Office of Science. The SDSS-III web site is <http://www.sdss3.org/>.

SDSS-III is managed by the Astrophysical Research Consortium for the Participating Institutions of the SDSS-III Collaboration including the University of Arizona, the Brazilian Participation Group, Brookhaven National Laboratory, Carnegie Mellon University, University of Florida, the French Participation Group, the German Participation Group, Harvard University, the Instituto de Astrofísica de Canarias, the Michigan State/Notre Dame/JINA Participation Group, Johns Hopkins University, Lawrence Berkeley National Laboratory, Max Planck Institute for Astrophysics, Max Planck Institute for Extraterrestrial Physics, New Mexico State University, New York University, Ohio State University, Pennsylvania State University, University of Portsmouth, Princeton University, the Spanish Participation Group, University of Tokyo, University of Utah, Vanderbilt University, University of Virginia, University of Washington, and Yale University.

The author acknowledges the use of computing resources of Universidad de los Andes, Bogotá, Colombia.

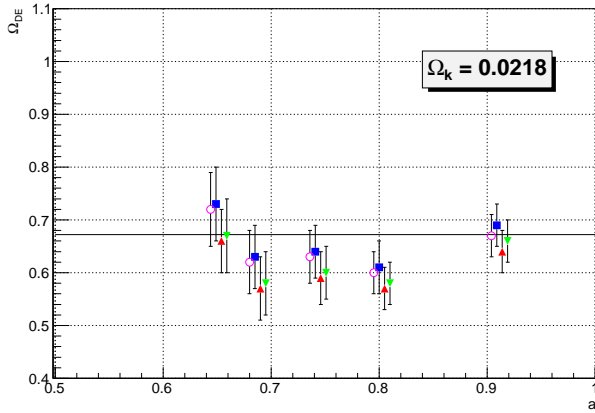


FIG. 3: Measurements of  $\Omega_{DE}(a)$  obtained from the 5  $\hat{d}_z(z, z_c)$  in Table III for  $\Omega_k = 0.0218$ , and the corresponding  $d_{BAO}$  and  $\Omega_{DE}$  from the fit for Scenario 1 in Table VII. The straight line is  $\Omega_{DE}(a) = 0.6723$  constant from the central value of this fit. The uncertainties correspond only to the total uncertainties of  $\hat{d}_z(z, z_c)$ . For clarity some offsets in  $a$  have been applied. We present results for  $(d_{BAO}, \Omega_{DE}) = (0.03383 - 0.00033, 0.6723)$  (squares),  $(0.03383 + 0.00033, 0.6723)$  (triangles),  $(0.03383, 0.6723 - 0.0068)$  (inverted triangles), and  $(0.03383, 0.6723 + 0.0068)$  (circles).

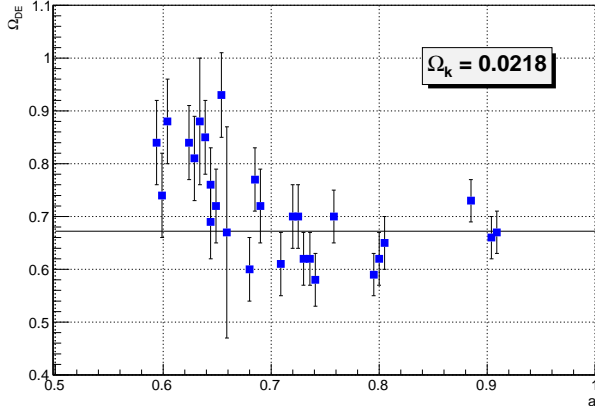


FIG. 4: Same as Figure 3 with the addition of the 6 measurements of  $\hat{d}_z(z, z_c)$  in Table III of Part I [2], and the 17 measurements of  $\hat{d}_z(z, z_c)$  in Table IV of Part I. These measurements are partially correlated. We present results for  $(d_{BAO}, \Omega_{DE}) = (0.03383, 0.6723)$ .

- 
- [1] Shadab Alam, et al. (SDSS-III), arXiv:1501.00963 (2015).
  - [2] B. Hoeneisen, arXiv:1607.02424 (2016).
  - [3] Shadab Alam et al., arXiv:1607.03155 (2016).
  - [4] Hee-Jong Seo, et al., ApJ, 720, 1650 (2010).
  - [5] B. Hoeneisen, arXiv:astro-ph/0009071 (2000).
  - [6] K.A. Olive et al. (Particle Data Group). Chin. Phys. C, 2014, **38**(9): 090001.
  - [7] D. J. Eisenstein, H.-J. Seo, and M. White, ApJ, 664: 660-674 (2007).
  - [8] E.M.L. Humphreys et al., Astrophys. J., 775, 13 (2013).